

## Transition to irreversibility in sheared suspensions: An analysis based on a mesoscopic entropy production

I. Santamaría-Holek,<sup>1</sup> G. Barrios,<sup>1</sup> and J. M. Rubi<sup>2</sup><sup>1</sup>*Facultad de Ciencias, Universidad Nacional Autónoma de México, Circuito exterior de Ciudad Universitaria, 04510 Distrito Federal, Mexico*<sup>2</sup>*Facultat de Física, Universitat de Barcelona, Av. Diagonal 647, 08028 Barcelona, Spain*

(Received 2 July 2008; revised manuscript received 9 October 2008; published 6 March 2009)

We study the shear-induced diffusion effect and the transition to irreversibility in suspensions under oscillatory shear flow by performing an analysis of the entropy production associated with the motion of the particles. We show that the Onsager coupling between different contributions to the entropy production is responsible for the scaling of the mean square displacement on particle diameter and applied strain. We also show that the shear-induced effective diffusion coefficient depends on the volume fraction, and use lattice-Boltzmann simulations to characterize the effect through the power spectrum of particle positions for different Reynolds numbers and volume fractions. Our study gives a thermodynamic explanation of the transition to irreversibility through a pertinent analysis of the second law of thermodynamics.

DOI: [10.1103/PhysRevE.79.031201](https://doi.org/10.1103/PhysRevE.79.031201)

PACS number(s): 66.10.cg, 82.70.Kj, 83.80.Hj, 87.15.Vv

### I. INTRODUCTION

When a suspension of non-Brownian particles is subjected to an oscillatory shear flow, the dynamics of the particles presents a transition to irreversibility which has been recently observed in experiments [1–3]. In these experiments, the suspension of polymethylmethacrylate particles having sufficiently large sizes (diameter  $d \approx 230 \mu\text{m}$ ) is contained in a cylindrical Couette cell and taken out of equilibrium by applying an oscillating shear flow proportional to  $\dot{\gamma} \cos(\omega t)$ , where  $\dot{\gamma} = \omega \gamma_0$  with  $\gamma_0$  the applied strain and  $\omega$  the characteristic frequency of the oscillation. At small enough Reynolds numbers it is observed that the motion of the particles is oscillatory and reversible, according to a classical result of hydrodynamics [4]. When increasing the Reynolds number or the concentration of particles, the trajectories of the particles become chaotic and then their reversible behavior is lost. This effect is manifested through a shear-induced diffusion which has been characterized through the mean square displacement (MSD) of the particles [1,2,5]. The MSD scales in the form  $\langle \Delta x^2 \rangle \sim d^2 \dot{\gamma} t$ , and thus allows one to define an effective diffusivity scaling as  $D \sim d^2 \dot{\gamma}$ .

Characterizing the motion of the particles through the MSD clearly suggests that a statistical description of their dynamics is possible. Previously, this description was offered in Ref. [5] by postulating a diffusion equation in which the diffusivities were constructed by analyzing the temporal behavior of the position correlation function of the particles. This approach allows the use of direct experimental measurements or simulation results in order to describe particular systems [3]. Other theoretical and numerical studies have characterized the relation between the transition to a chaotic motion of the particles with the shear-induced diffusion effect [1,2,5,6].

In this paper, we offer a general description of this shear-induced diffusion effect and the associated transition to irreversibility which is based on the application of the second law of thermodynamics, and on previous works devoted to analyze the dynamics of a suspension of Brownian particles

in the presence of flows [7,8]. We calculate the entropy production of the system in the phase space of the particles and find the corresponding Onsager couplings [7–9]. One of these couplings is responsible for the dependence of the diffusion tensor on the imposed velocity gradient, even in the limit of small specific thermal energy,  $k_B T/m \rightarrow 0$ , with  $k_B T$  the thermal energy and  $m$  the mass of a particle [7]. This dependence of the diffusion tensor on the velocity gradient leads to the shear-induced diffusion effect that depends crucially on hydrodynamic interactions [10–14], and the breaking of the fluctuation-dissipation relation at the mesoscopic level [7,15–22].

The paper is organized as follows. In Sec. II we use non-equilibrium thermodynamics in phase space to formulate the mesoscopic model based on a Fokker-Planck equation. Section III is devoted to deriving a Smoluchowski equation having an effective diffusion tensor accounting for the shear-induced diffusion observed in experiments. In Sec. IV we present lattice-Boltzmann simulations characterizing the shear-induced diffusion effect via the power spectrum of particle movements affected by hydrodynamic interactions. Finally, in Sec. V we discuss our main results.

### II. MESOSCOPIC ENTROPY PRODUCTION FOR THE DYNAMICS OF A SUSPENSION IN EXTERNAL FLOW

We consider a suspension of  $N$  noninteracting spherical particles of radius  $a$  and mass  $m$  in a fluid which moves with velocity  $\vec{v}^0(\vec{r}, t)$ . Since the system is in contact with a heat bath that evolves in time, it is necessary to determine the physical nature of the coupling forces in order to adequately describe its dynamics. This objective can be achieved by taking into account two factors. The first one is that the evolution of the system can be described at the mesoscopic level by means of the normalized  $N$ -particle probability distribution function  $P^{(N)}(\Gamma^N, t)$ , which depends on the instantaneous positions  $\{\vec{r}\}^N \equiv (\vec{r}_1, \dots, \vec{r}_N)$  of the particles and their velocities  $\{\vec{u}\}^N \equiv (\vec{u}_1, \dots, \vec{u}_N)$  through the phase space vector  $\Gamma^N$

$=(\{\vec{r}\}^N, \{\vec{u}\}^N)$ . The second factor takes into account the fact that the interactions between the system and the heat bath involve dissipation. This suggests the use of the nonequilibrium entropy  $s(t)$  as a thermodynamic potential from which the entropy production  $\sigma(t)$  can be calculated, and used to obtain the explicit expressions for the coupling forces [23].

To proceed in a systematic way, we will first notice that the probability distribution function satisfies the conservation law

$$\frac{\partial P^{(N)}}{\partial t} + \sum_{i=1}^N \vec{u}_i \cdot \vec{\nabla}_{\vec{r}_i} P^{(N)} = - \sum_{i=1}^N \frac{\partial}{\partial \vec{u}_i} \cdot \vec{J}_{\vec{u}_i}, \quad (1)$$

where  $\vec{\nabla}_{\vec{r}_i}$  represents the gradient operator with respect to the position vector  $\vec{r}_i$  and  $\vec{J}_{\vec{u}_i}$  is a diffusion current defined in phase space. Integration of Eq. (1) over the phase space coordinates  $\Gamma^N$ , under the assumption that  $P^{(N)}$  and  $\vec{J}_{\vec{u}_i}$  vanish at the boundaries, leads to the continuity equation:  $\partial \rho / \partial t = -\vec{\nabla} \cdot (\rho \vec{v})$  in which the average density field  $\rho(\vec{r}, t)$  of the suspended particles is defined by [14]

$$\rho(\vec{r}, t) = m \int \sum_{i=1}^N P^{(N)}(\Gamma^N, t) \delta(\vec{r}_i - \vec{r}) d\Gamma^N, \quad (2)$$

and the mean velocity field  $\vec{v}(\vec{r}, t)$  is

$$\vec{v}(\vec{r}, t) = \frac{1}{\rho} m \int \sum_{i=1}^N \vec{u}_i P^{(N)}(\Gamma^N, t) \delta(\vec{r}_i - \vec{r}) d\Gamma^N. \quad (3)$$

Here  $d\Gamma^N = d\{\vec{u}\}^N d\{\vec{r}\}^N$  is the volume element in the phase space of the particles.

One of the purposes of this section is to derive explicit expressions for the currents  $\vec{J}_{\vec{u}_i}$  which at this point implicitly contain the mentioned coupling forces between the system and bath. Once these expressions are obtained, the evolution equation for  $P^{(N)}$  can be written. As we have mentioned,  $\vec{J}_{\vec{u}_i}$  can be obtained from the entropy production of the system which follows from the Gibbs entropy postulate [14]

$$\delta s(t) = -k_B \int \sum_{i=1}^N P^{(N)} \ln \frac{P^{(N)}}{P_{LE}^{(N)}} \delta(\vec{r}_i - \vec{r}) d\Gamma^N, \quad (4)$$

where  $\delta s$  is the entropy change with respect to a local equilibrium (LE) reference state characterized by the local equilibrium distribution function

$$P_{LE}^{(N)} = \exp \left[ \frac{m}{k_B T} \left( \mu_B - \sum_{i=1}^N \frac{1}{2} (\vec{u}_i - \vec{v}_i^0)^2 \right) \right]. \quad (5)$$

Here  $\mu_B$  is the local equilibrium chemical potential per mass unit and  $\vec{v}_i^0 = \vec{v}^0(\vec{r}_i, t)$ .

Following the rules of mesoscopic nonequilibrium thermodynamics [9], we take the time derivative of Eq. (4) and use (1), an integration by parts over  $\Gamma^N$  space, assuming that the fluxes vanish at the boundaries, leads to a balance equation for the entropy  $s$  in which the entropy production contains three contributions:  $\sigma = \sum_{j=1}^3 \sigma_j$ . The first contribution is related to the diffusion process in  $\{\vec{u}\}$  space,

$$\sigma_1 = - \frac{m}{T} \int \sum_{i=1}^N \vec{J}_{\vec{u}_i} \cdot \frac{\partial \mu}{\partial \vec{u}_i} \delta(\vec{r}_i - \vec{r}) d\Gamma^N, \quad (6)$$

where the nonequilibrium chemical potential  $\mu(\Gamma^N, t)$  is given by

$$\mu(\Gamma^N, t) = \frac{k_B T}{m} \ln P^{(N)} + \frac{m}{2} \sum_{i=1}^N (\vec{u}_i - \vec{v}_i^0)^2. \quad (7)$$

The second contribution comes from diffusion of particles with respect to the mean velocity, with diffusion current  $\vec{J}_i = (\vec{u}_i - \vec{v}_i^0) P^{(N)}$ :

$$\sigma_2 = - \frac{m}{2T} \int \sum_{i=1}^N \vec{J}_i \cdot \vec{\nabla}_{\vec{r}_i} (\vec{u}_i - \vec{v}_i^0)^2 \delta(\vec{r}_i - \vec{r}) d\Gamma^N. \quad (8)$$

The third contribution corresponds to diffusion with respect to the flow velocity, whose current is  $\vec{J}_i^0 = (\vec{u}_i - \vec{v}_i^0) P^{(N)}$ ,

$$\sigma_3 = - \frac{m}{T} \int \sum_{i=1}^N \vec{J}_i^0 \cdot \vec{F}_i \delta(\vec{r}_i - \vec{r}) d\Gamma^N, \quad (9)$$

where  $\vec{F}_i = \partial \vec{v}_i^0 / \partial t$  is a nonstationary force related to the variation of the fluid velocity with time.

According to the second law of thermodynamics, the entropy production of the system must be positive definite  $\sigma > 0$  for irreversible process. To satisfy this condition, nonequilibrium thermodynamics establishes linear relationships between currents and forces [23]. In particular, for  $\vec{J}_{\vec{u}_i}$  we obtain

$$\begin{aligned} \vec{J}_{\vec{u}_i} = & - \sum_{j=1}^N P^{(N)} \vec{\alpha}_{ij} \cdot \frac{\partial \mu}{\partial \vec{u}_j} - \sum_{j=1}^N P^{(N)} \vec{\epsilon}_{ij} \cdot (\vec{u}_j - \vec{v}_j^0) \cdot \vec{\nabla}_{\vec{r}_j} \vec{v}_j^0 \\ & + \sum_{j=1}^N P^{(N)} \vec{\zeta}_{ij} \cdot \vec{F}_j, \end{aligned} \quad (10)$$

where the tensors  $\vec{\alpha}_{ij}$ ,  $\vec{\epsilon}_{ij}$ , and  $\vec{\zeta}_{ij}$  are related to the Onsager coefficients  $\vec{L}_{u,u_j}$ ,  $\vec{L}_{u,r_j}$ , and  $\vec{L}_{u,v_j}$  in the form [14]

$$\vec{\alpha}_{ij} = \vec{L}_{u,u_j} / TP^{(N)}, \quad \vec{\epsilon}_{ij} = \vec{L}_{u,r_j} / TP^{(N)}, \quad \vec{\zeta}_{ij} = \vec{L}_{u,v_j} / TP^{(N)}. \quad (11)$$

The Onsager coefficients obey Onsager's relations in which time-reversal symmetry must also be applied to the external drive:  $\vec{L}_{u,r_j} = -\vec{L}_{r,u_j}$ , [24]. From Eq. (10) it follows that the system of particles is coupled to the heat bath by means of thermal and entropic forces (first term on the right-hand side of the equation) and mechanical forces (last two terms of the equation).

Substituting Eq. (10) into the continuity equation for the probability (1), we arrive at the multivariate Fokker-Planck equation describing the evolution of the  $N$ -particle distribution function,

$$\begin{aligned}
 \frac{\partial P^{(N)}}{\partial t} + \sum_{i=1}^N \nabla_{\vec{r}_i} \cdot (\vec{u}_i P^{(N)}) \\
 = \sum_{i,j=1}^N \frac{\partial}{\partial \vec{u}_i} \cdot \left( [(\vec{u}_j - \vec{v}_j^0) \cdot \vec{\beta}_{ij} - \vec{\zeta}_{ij} \cdot \vec{F}_j] P^{(N)} \right. \\
 \left. + \frac{k_B T}{m} \vec{\alpha}_{ij} \cdot \frac{\partial P^{(N)}}{\partial \vec{u}_j} \right), \quad (12)
 \end{aligned}$$

where we have used Eqs. (7) and (10) assuming that the coefficients are symmetric tensors. Finally we introduced the friction tensor  $\vec{\beta}_{ij}$ , leading to the relation [7]

$$\vec{\alpha}_{ij} = \vec{\beta}_{ij} - \vec{\epsilon}_{ij} \cdot \vec{\nabla}_{\vec{r}_j} \vec{v}_j^0. \quad (13)$$

It is important to mention that the combination  $\vec{\epsilon}_{ij} \cdot \vec{\nabla}_{\vec{r}_j} \vec{v}_j^0$ , entering in Eqs. (12) and (13), implies that the fluctuation-dissipation theorem connecting the drift and diffusion terms of the Fokker-Planck equation is no longer valid due to the presence of the shear [7,15,16,22]. This important consequence following from Eq. (12) is related to the shear-induced diffusion effect, as we will show in the next section. In the case of a diluted suspension, similar results for the diffusion term of the generalized Fokker-Planck equation have been obtained by means of the kinetic theory of gases in Ref. [21].

The coefficient  $\vec{\epsilon}_{ij}$  is related to the force exerted on the surface of a particle moving through a fluid under flow conditions. For a spherical particle,  $\vec{\epsilon}_{ij}$  has been calculated explicitly in terms of the generalized Faxén theorem in Ref. [25], and used in Ref. [8] to obtain  $\vec{\epsilon}_{ij} = \epsilon_0 \vec{\tilde{\epsilon}}_{ij}$  with

$$\epsilon_0 = \frac{1}{6} \frac{m}{k_B T} a^2 \beta_0^2 (1 + 2a\alpha), \quad (14)$$

where  $\beta_0 = 6\pi\eta a/m$  is the Stokes friction coefficient per mass unit and  $\eta$  the viscosity of the fluid,  $\alpha = (-i\omega/\nu)^{1/2}$  is the inverse viscous penetration length,  $\omega$  is the frequency and  $\nu$  the corresponding kinematic viscosity [8,25]. The tensor  $\vec{\tilde{\epsilon}}_{ij}$  is related to the friction tensor  $\vec{\beta}_{ij}$  and obeys the relation  $\vec{\tilde{\epsilon}}_{ii} = \vec{1}$  with  $\vec{1}$  the unit tensor. In Ref. [8] it has been shown that  $\vec{\tilde{\zeta}}_{ij}$  is related to inertial effects due to the change in time of  $\vec{v}_0$  and has the form  $\vec{\tilde{\zeta}}_{ij} = \zeta \vec{1} \delta_{ij}$ , with  $\zeta = \rho_p/\rho_f$ ,  $\rho_p$  the density of the particle, and  $\rho_f$  the density of the heat bath. From Eq. (14) it follows that  $\epsilon_0$  incorporates finite-size effects on the dynamics of the system through the surface term  $a^2$  and frequency-dependent corrections to the diffusion coefficient through  $\alpha$ .

Equations (12)–(14) imply that the diffusion coefficient in velocity space,  $(k_B T/m) \vec{\alpha}_{ij}$ , does not vanish in the limit  $k_B T/m \rightarrow 0$  and, therefore, also imply that the nonthermal contribution to the diffusion coefficient associated with the Onsager coefficient  $\epsilon_{ij}$  may have important consequences for the dynamics of a non-Brownian suspension of particles. We will show these consequences in the next section.

The friction tensors  $\vec{\beta}_{ij}$  are affected by the hydrodynamic interactions among particles and their dependence can be inferred from its relation with the mobility tensors  $\vec{\mu}_{ij}$ :  $\vec{\beta}_{ij} \cdot \vec{\mu}_{ij} = \vec{1} \delta_{ij}$ . At a lower-order approximation, the multipole expansion of  $\vec{\mu}_{ij}$  takes the form [11]

$$\begin{aligned}
 \vec{\mu}_{ij} \approx \beta_0^{-1} \vec{1} \delta_{ij} + \beta_0^{-1} \left( \frac{3}{4} \frac{a}{r_{ij}} (\vec{1} + \hat{r}_{ij} \hat{r}_{ij}) (1 - \delta_{ij}) \right. \\
 \left. - \frac{3}{4} \frac{a}{r_{ij_s}} (\vec{1} + \hat{r}_{ij_s} \hat{r}_{ij_s}) \right). \quad (15)
 \end{aligned}$$

Here  $\hat{r}_{ij}$  and  $\hat{r}_{ij_s}$  are the unit relative vectors between particles and between particle  $j$  and the wall.  $\vec{r}_{ij} = \vec{r}_i - \vec{r}_j$  is distance between particles whereas  $r_{ij_s}$  is the magnitude of the vector that points from sphere  $i$  to the mirror image with respect to a wall of sphere  $j$ . For  $i=j$ , Eq. (15) reduces to well-known results for the mobility of a particle in the presence of a wall:  $\mu = \beta_0^{-1} (1 - B_1 a/l)$ , with  $l$  its distance to the wall. The coefficient  $B_1$  may take different values depending on the direction of the motion of the particle with respect to the plane of the wall [26].

### III. SHEAR-INDUCED DIFFUSION

We will analyze in this section the diffusion regime occurring at times  $t \gg \beta_0^{-1}$ . Since experiments and simulations give the self-diffusion coefficient [1,27], we will focus our description on the dynamics of a single particle whose reduced distribution function  $\rho_k(\vec{r}, t) = m \int P^{(N)} \delta(\vec{r}_k - \vec{r}) d\Gamma^N$  satisfies the continuity equation

$$\frac{\partial \rho_k}{\partial t} = - \vec{\nabla} \cdot (\rho_k \vec{v}_k), \quad (16)$$

which follows by integrating Eq. (12) over the phase space of the particles and where  $\vec{v}_k(\vec{r}, t) = m \rho_k^{-1} \int \vec{u}_k P^{(N)} \delta(\vec{r}_k - \vec{r}) d\Gamma^N$ .

The Smoluchowski equation for  $\rho_k$  can be derived after calculating the explicit expression for  $\rho_k \vec{v}_k$ . This task can be carried out by calculating the evolution equations for the momentum field  $\rho_k \vec{v}_k$  and for the pressure tensor of the  $k$ th particle, defined as

$$\vec{P}_k(\vec{r}, t) = m \int (\vec{u}_k - \vec{v}_k) (\vec{u}_k - \vec{v}_k) P^{(N)} \delta(\vec{r}_k - \vec{r}) d\Gamma^N. \quad (17)$$

Following the method indicated in Ref. [7], we take the time derivative of the definition of  $\rho_k(\vec{r}, t)$ , use Eq. (12) in the result, and perform an integration by parts assuming that the currents vanish at the boundaries. After rearranging terms we arrive at the equation

$$\begin{aligned}
 \rho_k \frac{d_k}{dt} \vec{v}_k + \vec{\nabla} \cdot \vec{P}_k = - \int \sum_{i=1}^N \vec{\beta}_{ki} \cdot (\vec{v}_i^{(2)} - \vec{v}_i^0) \rho^{(2)} \delta(\vec{r}_k - \vec{r}) d\vec{r}_k d\vec{r}_i \\
 + \rho \zeta \vec{F}, \quad (18)
 \end{aligned}$$

where we have used the expression  $\vec{\zeta}_{ij} = \zeta \vec{1} \delta_{ij}$  and defined the convective derivative  $d_k/dt = \partial/\partial t + \vec{v}_k \cdot \partial/\partial \vec{r}$ , and the

two-particle reduced distribution function  $\rho^{(2)}(\vec{r}_k, \vec{r}_i, t) = m \int P^{(N)} d\Gamma_{ki}^{N-2}$ . Here,  $d\Gamma_{ki}^{N-2}$  is the phase-space volume element of the  $N-2$  particles including the measure associated to the velocities  $\vec{u}_k$  and  $\vec{u}_i$ . In  $\vec{v}_i^{(2)}$  the superscript indicates a dependence on  $\vec{r}_k$  and  $\vec{r}_i$ . The right-hand side of Eq. (18) represents the total drag force exerted by the fluid on the particles. The first term on the right-hand side is the friction force including the presence of hydrodynamic interactions that modifies the local value of the velocity field in terms of the distribution of particles in the system.

The evolution equation for the pressure tensor  $\vec{P}_k$  can be derived by following a similar procedure:

$$\begin{aligned} \frac{d_k \vec{P}_k}{dt} + 2 \left[ \left( \beta_0 \vec{1} + \nabla \vec{v}_k + \frac{1}{2} \vec{\nabla} \cdot \vec{v}_k \vec{1} \right) \cdot \vec{P}_k \right]^s \\ = \frac{2k_B T}{m} \beta_0 \rho_k \left( \vec{1} - \frac{m}{6k_B T} a^2 \beta_0 (1 + 2a\alpha) \vec{\nabla} \vec{v}_k^0 \right)^s \\ - 2 \left( \int \sum_{i=1, i \neq k}^N \vec{\beta}_{ki} \cdot (\vec{v}_k^{(2)} - \vec{v}_k^0) (\vec{v}_i^{(2)} - \vec{v}_i^0) \right. \\ \left. \times \rho^{(2)} \delta(\vec{r}_k - \vec{r}) d\vec{r}_k d\vec{r}_i \right)^s, \end{aligned} \quad (19)$$

where, to obtain the second term on the right-hand side, we have used the expressions (13) and (14) for  $i=j$ . The upper symbol  $s$  means the symmetric part of a tensor. The last term on the right-hand side of this equation contains the contribution of the hydrodynamic interactions to the pressure tensor of the particle  $k$ . This contribution enters through the cross-correlation functions of the local velocities indicating how hydrodynamic interactions modify the stresses in the system. In order to obtain a closed expression for the pressure tensor  $\vec{P}_k$ , it thus becomes necessary to calculate the evolution equation for the cross-correlation function

$$\vec{C}_{ki}(\vec{r}, t) = \int (\vec{u}_k - \vec{v}_k) (\vec{u}_i - \vec{v}_i) P^{(N)} \delta(\vec{r}_k - \vec{r}) d\Gamma^N. \quad (20)$$

The evolution equation for  $\vec{C}_{ki}$  can be obtained in a similar way as we did to derive Eq. (19). The result is

$$\begin{aligned} \frac{d_k \vec{C}_{ki}}{dt} + 2 \left[ \left( \vec{\nabla} \vec{v}_k + \frac{1}{2} \vec{\nabla} \cdot \vec{v}_k \vec{1} \right) \cdot \vec{C}_{ki} \right]^s \\ = \frac{2k_B T}{m} \int \sum_{j=1}^N \vec{\alpha}_{kj}^s \delta_{ji} \rho^{(2)} \delta(\vec{r}_k - \vec{r}) d\vec{r}_k d\vec{r}_i \\ - 2 \left( \int \sum_{j=1}^N \vec{\beta}_{kj} \cdot (\vec{v}_j^{(2)} - \vec{v}_j^0) (\vec{v}_i^{(2)} - \vec{v}_i^0) \rho^{(2)} \delta(\vec{r}_k - \vec{r}) d\vec{r}_k d\vec{r}_i \right)^s, \end{aligned} \quad (21)$$

where  $k \neq i$ . To derive Eqs. (20) and (21), we have neglected the contributions arising from higher-order moments of the time-ordered hierarchy since they relax faster than the ones present in those equations [7].

At times  $t \gg \beta_0^{-1}$ , we can obtain from (19) the following constitutive equation for  $\vec{P}_k$ :

$$\begin{aligned} \vec{P}_k \approx \frac{k_B T}{m} \rho_k \left( \vec{1} - \frac{m}{6k_B T} a^2 \beta_0 (1 + 2a\alpha) \nabla \vec{v}_k^0 \right)^s \\ - \left( \beta_0^{-1} \int \sum_{i=1, i \neq k}^N \vec{\beta}_{ki} \cdot (\vec{v}_k^{(2)} - \vec{v}_k^0) (\vec{v}_i^{(2)} - \vec{v}_i^0) \right. \\ \left. \times \rho^{(2)} \delta(\vec{r}_k - \vec{r}) d\vec{r}_k d\vec{r}_i \right)^s, \end{aligned} \quad (22)$$

where we have used that  $(\vec{\nabla} \vec{v}_k)_{ij} \beta_0^{-1} \ll 1$ ,  $\vec{\nabla} \cdot \vec{v}_k \beta_0^{-1} \ll 1$ , in accordance with the experiments [1]. For times  $t \gg \beta_0^{-1}$ , Eq. (21) can be rewritten in similar form as Eq. (22) by extracting the term  $j=k$  from the sum on the second term at the right-hand side, multiplying the resulting relation by  $\beta_0^{-1} \vec{\beta}_{ki}$  and performing the sum over  $i$ . One obtains the expression

$$\begin{aligned} \frac{k_B T}{m} \beta_0^{-1} \int \sum_{i=1, i \neq k}^N \vec{\beta}_{ki} \cdot \vec{\alpha}_{ki} \rho^{(2)} \delta(\vec{r}_k - \vec{r}) d\vec{r}_k d\vec{r}_i \\ \approx \int \sum_{i=1, i \neq k}^N \vec{\beta}_{ki} \cdot (\vec{v}_k^{(2)} - \vec{v}_k^0) (\vec{v}_i^{(2)} - \vec{v}_i^0) \rho^{(2)} \delta(\vec{r}_k - \vec{r}) d\vec{r}_k d\vec{r}_i, \end{aligned} \quad (23)$$

where we have used  $\vec{\beta}_{kk} = \beta_0 \vec{1}$ , kept terms of the order  $(a/r_{ij})^2$ , and neglected terms of the order  $(a/r_{ij})^4$  and higher. This approximation is valid up to intermediate volume fractions of the suspended particles.

### A. Effective medium approximation

The Smoluchowski equation for  $\rho_k$  can be obtained from (16), (18), (22), and (23) by assuming an effective medium approximation in which the test particle  $k$  performs its motion in a fluid incorporating the effects of hydrodynamic interactions in average form [28]. In our description, this assumption does not consider the possibility of direct collisions among particles, and thus we expect that it is valid up to intermediate volume fractions of the suspended particles. Operationally, this approximation can be implemented by substituting the averages appearing on the right-hand sides of Eqs. (18), (22), and (23) by integrals over a continuum variable. Thus, the last term on the right-hand side of Eqs. (22) and (23) may be written as

$$\begin{aligned} \int \sum_{i=1, i \neq k}^N \vec{\beta}_{ki} \cdot (\vec{v}_k^{(2)} - \vec{v}_k^0) (\vec{v}_i^{(2)} - \vec{v}_i^0) \rho^{(2)} \delta(\vec{r}_k - \vec{r}) d\vec{r}_k d\vec{r}_i \\ \approx \int \vec{\beta}(\vec{r}') \cdot \vec{C}^*(\vec{r} - \vec{r}', t) d\vec{r}', \end{aligned} \quad (24)$$

where we have introduced the nonlocal velocity cross-correlation function  $\vec{C}^*(\vec{r} - \vec{r}', t)$ . In similar form, for the momentum field we have the relation

$$\begin{aligned} & \int \sum_{i=1, i \neq k}^N \vec{\beta}_{ki} \cdot (\vec{v}_i^{(2)} - \vec{v}_i^0) \rho^{(2)} \delta(\vec{r}_k - \vec{r}) d\vec{r}_k d\vec{r}_i \\ & \simeq \int \vec{\beta}(\vec{r}') \cdot (\vec{v} - \vec{v}^0)_{\vec{r}, \vec{r}'} \rho^{(2)}(\vec{r} - \vec{r}', t) d\vec{r}', \end{aligned} \quad (25)$$

where we have defined  $(\vec{v} - \vec{v}^0)_{\vec{r}, \vec{r}'} \equiv \vec{v}(\vec{r} - \vec{r}', t) - \vec{v}^0(\vec{r} - \vec{r}', t)$ . Using Eqs. (13) and (14), the right-hand side of Eq. (23) can be rewritten as

$$\begin{aligned} & \int \sum_{i=1, i \neq k}^N \vec{\beta}_{ki} \cdot \vec{\alpha}_{ki}^* \rho^{(2)} \delta(\vec{r}_k - \vec{r}) d\vec{r}_k d\vec{r}_i \\ & = \int \vec{\alpha}^*(\vec{r}') \rho^{(2)}(\vec{r} - \vec{r}', t) d\vec{r}' \\ & = \int \vec{\beta}(\vec{r}') \cdot \vec{\beta}(\vec{r}') \rho^{(2)}(\vec{r} - \vec{r}', t) d\vec{r}' - \frac{m}{6k_B T} a^2 \beta_0^2 (1 + 2a\alpha) \\ & \quad \times (\vec{\nabla} \vec{v}^0)^\dagger \cdot \int [\vec{\beta}(\vec{r}') \cdot \vec{\epsilon}(\vec{r}')]^\dagger \rho^{(2)}(\vec{r} - \vec{r}', t) d\vec{r}', \end{aligned} \quad (26)$$

where the superscript  $\dagger$  means the transpose of a tensor and we have used the fact that  $\vec{\nabla} \vec{v}^0$  does not depend on position. The tensor  $\vec{\alpha}^*(\vec{r}') = \vec{\beta}(\vec{r}') \cdot \vec{\alpha}(\vec{r}')$  has been defined to simplify the notation in subsequent relations. In the long-time limit the substitution of Eqs. (24) and (26) into (22) yields the constitutive equation for the pressure tensor,

$$\begin{aligned} \vec{P} & \simeq \frac{k_B T}{m} \left[ \rho \left( \vec{1} - \frac{m}{6k_B T} a^2 \beta_0 (1 + 2a\alpha) \vec{\nabla} \vec{v}^0 \right) \right. \\ & \quad \left. - \beta_0^{-2} \int \vec{\alpha}^*(\vec{r}') \rho^{(2)}(\vec{r} - \vec{r}', t) d\vec{r}' \right]^s, \end{aligned} \quad (27)$$

where we have assumed that the second term on the left-hand side of Eq. (21) may be neglected [see Eq. (22)].

Using now Eq. (25) in (18) and taking the long-time limit  $t \gg \beta_0^{-1}$ , from the momentum equation we obtain

$$\vec{\nabla} \cdot \vec{P} \simeq - \int \vec{\beta}(\vec{r}') \cdot (\vec{v} - \vec{v}^0)_{\vec{r}, \vec{r}'} \rho^{(2)}(\vec{r} - \vec{r}', t) d\vec{r}' + \rho \zeta \vec{F}. \quad (28)$$

The explicit expression for the constitutive relation of the diffusion current  $\rho \vec{v}$  of the particles follows by assuming that the spatial variation of the velocity field is small enough in order to make the expansion

$$\vec{v}(\vec{r} - \vec{r}', t) - \vec{v}^0(\vec{r} - \vec{r}', t) \simeq \vec{v}(\vec{r}) - \vec{v}^0(\vec{r}) + O((\vec{\nabla} \vec{v}^0)^2), \quad (29)$$

where we have used  $\vec{v} \simeq \vec{v}^0 + O(\vec{\nabla} \ln \rho)$  [7].

Factorizing the two-particle distribution function in the form [29]  $\rho^{(2)}(\vec{r} - \vec{r}', t) \simeq \rho(\vec{r}') g(\vec{r} - \vec{r}', t)$ , with  $g(\vec{r} - \vec{r}', t)$  the two-particle correlation function, we define the effective quantities

$$\vec{B}(\vec{r}, t; \phi) = \beta_0^{-1} \int \vec{\beta}(\vec{r}') \cdot \vec{\beta}(\vec{r}') g(\vec{r} - \vec{r}', t; \phi, T) d\vec{r}' \quad \text{and} \quad (30)$$

$$\vec{E}(\vec{r}, t; \phi) = \beta_0^{-1} \int \vec{\beta}(\vec{r}') \cdot \vec{\epsilon}(\vec{r}') g(\vec{r} - \vec{r}', t; \phi, T) d\vec{r}',$$

where we have taken into account the fact that the two-particle correlation function  $g$  may in general depend on the volume fraction and the temperature [30].

After using these results in Eqs. (26)–(28), we obtain the following constitutive equation for the diffusion current:

$$\rho \vec{v} \simeq \rho \vec{v}^0 - \frac{k_B T}{m} \vec{B}^{-1} \cdot (\vec{\nabla} \cdot \vec{A}) \rho + \rho \zeta \vec{B}^{-1} \cdot \vec{F} - \vec{D}(\vec{r}, t) \cdot \vec{\nabla} \rho, \quad (31)$$

where we have identified the effective diffusion tensor

$$\vec{D}(\vec{r}, t) = (k_B T/m) \vec{\mu} + \frac{a^2}{6} (1 + 2a\alpha) [(\vec{1} + \vec{\mu}) \cdot (\vec{E} - \vec{1}) \cdot \vec{\nabla} \vec{v}^0]^s. \quad (32)$$

Here  $\vec{\mu} = \beta_0^{-1} \vec{\mu}$  is the effective mobility tensor and we have introduced the dimensionless tensors

$$\vec{\mu} = \beta_0 \vec{B}^{-1} - \vec{1} \quad \text{and} \quad (33)$$

$$\vec{A} = \left( \vec{1} - \beta_0^{-1} \vec{B} + \frac{m}{6k_B T} a^2 \beta_0 (1 + 2a\alpha) (\vec{E} - \vec{1}) \cdot \vec{\nabla} \vec{v}^0 \right)^s.$$

Equations (30)–(32) show that the transport coefficients in the coarse-grained description contain hydrodynamic interactions in effective form through the configurationally averaged tensors  $\vec{B}$  and  $\vec{E}$ . When  $\vec{\nabla} \vec{v}^0 = \vec{0}$ , then the diffusion tensor reduces to  $\vec{D}(\vec{r}, t) = (k_B T/m) \vec{\mu}(\vec{r}, t; \phi)$ , that is, in equilibrium the diffusion tensor depends on hydrodynamic interactions through the mobility tensor  $\vec{\mu}$ , as expected. The coarse-graining performed in this section thus leads to incorporate the contribution of hydrodynamic interactions in the dissipation of the reduced system by modifying the diffusion coefficient making it anisotropic and position and time dependent. Substituting now Eq. (31) into (16), we finally obtain the Smoluchowski equation

$$\begin{aligned} \frac{\partial \rho}{\partial t} & = - \vec{\nabla} \cdot [\rho \vec{v}^0 - \rho \beta_0^{-1} (\vec{1} + \vec{\mu}) \cdot \vec{f} - \rho \zeta \beta_0^{-1} (\vec{1} + \vec{\mu}) \cdot \vec{F}] \\ & \quad + \vec{\nabla} \cdot (\vec{D} \cdot \vec{\nabla} \rho), \end{aligned} \quad (34)$$

where we have defined the force  $\vec{f}$  due to hydrodynamic interactions as  $\vec{f} = -(k_B T/m) \vec{\nabla} \cdot \vec{A}$ .

Equations (32)–(34) constitute the main result of this section. The *effective* diffusion tensor  $\vec{D}$  contains two contributions. The first one depends on the thermal energy per mass unit ( $k_B T/m$ ) and is therefore related to Brownian motion

whereas the second one does not depend on thermal fluctuations.

In the limit of vanishing specific thermal energy,  $k_B T/m \rightarrow 0$ , Eq. (32) leads to

$$\overset{\rceil}{D} = \frac{a^2}{6}(1 + 2a\alpha)[(\overset{\rceil}{1} + \overset{\rceil}{\mu}) \cdot (\overset{\rceil}{E} - \overset{\rceil}{1}) \cdot \nabla \vec{v}^0]^s. \quad (35)$$

This expression has the same scaling on particle diameter and shear rate as that observed in experiments and Stokesian dynamics simulations [1,27]. The presence of  $\overset{\rceil}{\mu}(\vec{r}, t; \phi)$  and  $\overset{\rceil}{E}(\vec{r}, t; \phi)$  implies that the shear-induced diffusion is mediated by hydrodynamic interactions. We then conclude that hydrodynamic interactions are responsible for the randomization in the motion of the suspended particles when an oscillatory strain is applied on the system.

### B. The mean square displacement

We will assume that the fluid velocity  $\vec{v}_0(\vec{r}, t) = \vec{r} \cdot \overset{\rceil}{\gamma}(t)$  is imposed along the  $x$  direction with  $\overset{\rceil}{\gamma}(t)$  the time-dependent shear rate whose only nonvanishing component is  $\gamma_{yx} = \dot{\gamma} \cos(\omega t)$ . The shear rate is related to the applied strain  $\gamma_0$  by  $\dot{\gamma} = \gamma_0 \omega$ . For convenience, we will assume that inertial effects are negligible and that effective mobility  $\overset{\rceil}{\mu}$  and  $\overset{\rceil}{E}$  do not depend on time and position. This hypothesis is valid when the distribution of the suspended particles does not change significantly, that is, when  $g(\vec{r}' - \vec{r}, t; \phi) \sim g(\vec{r}'; \phi)$ .

The MSD of the particle's position vector can be calculated by taking the time derivative of the expression

$$\langle r^2 \rangle = \int (x^2 + y^2) \rho d\vec{r}, \quad (36)$$

where we have considered the two-dimensional case. Substitution of Eq. (34) into the result and an integration by parts leads to

$$\frac{d}{dt} \langle r^2 \rangle = 2 \dot{\gamma} \cos(\omega t) \langle xy \rangle(t) + 2 \text{Tr}[\overset{\rceil}{D}], \quad (37)$$

where  $\langle xy \rangle(t) = \int xy \rho d\vec{r}$ . In similar form, we must derive the evolution equations for  $\langle xy \rangle(t)$ ,  $\langle x^2 \rangle(t)$ , and  $\langle y^2 \rangle(t)$ . After solving the obtained set of differential equations, for low shear rates and frequencies ( $\dot{\gamma} < 1$ ,  $\omega < 1$ ) we may expand the MSD in a power series of  $\dot{\gamma}$  and  $\omega$  to obtain

$$\langle r^2 \rangle \simeq 4D_0(\overset{\rceil}{\mu}_{xx} + \overset{\rceil}{\mu}_{yy})t + \frac{1}{6} \overset{\rceil}{\mu}_{xy}(E-1)d^2 \dot{\gamma} t \left( 1 + \frac{24}{d^2(E-1)} D_0 t \right), \quad (38)$$

where  $D_0 = k_B T/m\beta_0$  is the one-particle diffusion coefficient and  $d=2a$ , having assumed  $\overset{\rceil}{\mu}_{xy} = \overset{\rceil}{\mu}_{yx}$  and  $\overset{\rceil}{E} = E\overset{\rceil}{1}$ . In the limit  $k_B T/m \rightarrow 0$  when the particles are non-Brownian we obtain

$$\langle r^2 \rangle \sim \frac{1}{6} \overset{\rceil}{\mu}_{xy}(\phi)[E(\phi) - 1]d^2 \dot{\gamma} t. \quad (39)$$

When Eq. (39) is expressed in terms of the number of oscillations  $n$  of the imposed flow, with  $t=2\pi n/\omega$ , it gives  $\langle r^2 \rangle$

$\sim (\pi/3) \overset{\rceil}{\mu}_{xy}(E-1)d^2 \gamma_0 n$ . This relation shows that hydrodynamic interaction introduce a volume fraction dependence to the MSD of the particle, thus giving an explanation based on thermodynamic arguments for the scaling relation obtained in the experiments [1].

In the limit of massive particles, from Eq. (34) it is also possible to derive the evolution equation for the average position of the particle defined through  $\vec{R}(t) = \int \vec{r} \rho d\vec{r}$ . By taking the time derivative of this definition and integrating by parts one obtains

$$\begin{aligned} \frac{d}{dt} \vec{R}(t) &= \vec{R}(t) \cdot \nabla \vec{v}_0(t) - \zeta \beta_0^{-1} \overset{\rceil}{G}_1(\vec{R}; \phi) \cdot \frac{d}{dt} \nabla \vec{v}_0(t) \\ &+ \frac{a^2}{6} \overset{\rceil}{G}_2(\vec{R}; \phi) \cdot \nabla \vec{v}_0(t), \end{aligned} \quad (40)$$

where we have introduced the quantities  $\overset{\rceil}{G}_1 = \langle (\overset{\rceil}{1} + \overset{\rceil}{\mu}) \cdot \vec{r} \rangle$  and  $\overset{\rceil}{G}_2 = \langle \nabla \cdot [(\overset{\rceil}{1} + \overset{\rceil}{\mu}) \cdot (\overset{\rceil}{E} - \overset{\rceil}{1})] \rangle$  and the angular brackets indicate an average over  $\rho$ . Equation (40) is a nonlinear equation for  $\vec{R}(t)$  in which the nonlinearities are a consequence of hydrodynamic interactions through the terms  $\overset{\rceil}{G}_1$  and  $\overset{\rceil}{G}_2$ . In a first approximation, the last term at the right-hand side of Eq. (40) establishes that hydrodynamic interactions become significant when the Reynolds number defined by  $\text{Re} \equiv d v_0 / \nu$  satisfies the condition

$$\text{Re} > \frac{24d^2 \omega}{\nu} h(\phi), \quad (41)$$

where  $\nu$  is the kinematic viscosity of the heat bath and the function  $h(\phi)$  takes into account that  $(G_2)_{ij}$  is a function of  $\phi$ . In obtaining this relation we have neglected the second term at the right-hand side of (40) since  $\beta_0^{-1}$  is a very small quantity and scaled time with  $\omega$  and lengths with  $d$ . Equations (39) and (41) show that the transition to irreversibility is mediated by hydrodynamic interactions that introduce a dependence on volume fraction of the shear-induced diffusion coefficient.

### IV. SHEAR-INDUCED DIFFUSION FROM LATTICE-BOLTZMANN SIMULATIONS

In this section, we analyze the shear-induced diffusion effect by means of lattice-Boltzmann simulations. This method allows us to study the dependence of the effective diffusion coefficient as a function of the relevant parameters of the problem, the Reynolds number  $\text{Re}$  and the volume fraction  $\phi$ . The power spectrum of the components of the trajectories of the particles is used to show that the randomization of particle movements is due to an increasing number of modes produced by hydrodynamic interactions as  $\text{Re}$  and  $\phi$  increase.

We use the two-dimensional model D2Q9 for the lattice-Boltzmann method with the Bhatnagar-Gross-Krook (BGK) approximation [31,32]. In this model, the space is discretized in a two-dimensional square lattice with nine velocities ( $\mathbf{c}_i, i=0, \dots, 8$ ) allowed. The particle distribution functions  $f(\mathbf{r}, t)$  at site  $\mathbf{r}$  and time  $t$  evolve according to the equation

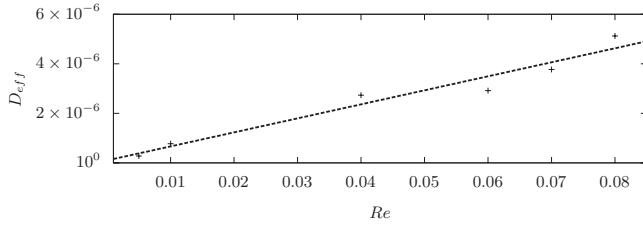


FIG. 1. Effective diffusion coefficient as a function of  $Re$  (symbols) for a fixed particle concentration of  $\phi=0.14$  and  $f^*=10.0$ . The solid line is a linear fit with slope of  $5.68 \times 10^{-5}$ .

$$f_i(\mathbf{r} + \Delta t \mathbf{c}_i, t + \Delta t) - f_i(\mathbf{r}, t) = -\frac{1}{\tau} [f_i(\mathbf{r}, t) - f_i^{(eq)}(\mathbf{r}, t)], \quad (42)$$

where  $\tau$  is the dimensionless relaxation time related to viscosity and  $f_i^{(eq)}$  are the local equilibrium distribution functions,

$$f_i^{(eq)} = w_i \rho \left( 1 + 3 \mathbf{c}_i \cdot \mathbf{u} + \frac{9}{2} (\mathbf{c}_i \cdot \mathbf{u})^2 - \frac{3}{2} u^2 \right). \quad (43)$$

In this equation,  $w_i=4/9, 1/9, 1/36$  are the weights associated with the lattice [33] for each set of velocities  $|\mathbf{c}_i|=0, 1, \sqrt{2}$  and  $\rho$  and  $\mathbf{u}$  are the density and velocity defined by

$$\rho(\mathbf{r}, t) = \sum_i f_i(\mathbf{r}, t), \quad \mathbf{u}(\mathbf{r}, t) = \frac{1}{\rho} \sum_i f_i(\mathbf{r}, t) \mathbf{c}_i. \quad (44)$$

The viscosity is related to the dimensionless relaxation time by  $\nu = c_s^2(\tau - 1/2)$ , where  $c_s = 1/\sqrt{3}$  is the speed of sound in the D2Q9 model.

The no-slip boundary conditions are simulated on the solid particles and the torques and forces are also evaluated to update the particle position at all times [34]. The interactions among particles are implemented with the method proposed in Ref. [35] and with the corrections proposed in Ref. [34]. The walls of the cavity use the bounce-back boundary condition, which consists in reversing the incoming particle distribution function after the streaming process.

The numerical simulations are carried out in a cavity of  $H^*=11.33$  and  $W^*=44.66$  where the dimensions are scaled with the radius of the particle. The relaxation time and the radius of the particles are kept constant in all simulations at  $\tau=20.0$ ,  $r=4.5$ , and  $f^*=10.0$  and we have varied the Reynolds number and the volume fraction. The dimensionless frequency was scaled with the magnitude of the shear rate.

In the first set of numerical simulations, we fixed the particle concentration  $\phi=0.14$  and the dimensionless frequency  $f^*=10$ , varied the Reynolds number, and determined the effective diffusion coefficient  $D_{\text{eff}}$  as shown in Fig. 1. A linear dependence of  $D_{\text{eff}}$  on  $Re$  has been obtained to a good approximation, as expected from experiments and theoretical results. Using the definition  $Re = d^2 \dot{\gamma} / \nu$ , from Eq. (39) we may also obtain the linear relation for the effective diffusivity as a function of the Reynolds number:  $D_{\text{eff}} = \tilde{\mu}_{xy}(\phi)[E(\phi)-1]\nu Re/6$ . The data obtained from simulations can be used to give a rough estimate of the magnitude

of hydrodynamic interactions in terms of the parameter  $\tilde{\mu}_{xy}(\phi)[E(\phi)-1]$ . Given  $d=9$  and  $\nu=11.25$  we obtain  $\tilde{\mu}_{xy}(\phi)[E(\phi)-1] \sim 10^{-4}$ . This small value indicates that three-dimensional (3D) lattice-Boltzmann simulations are required in order to do a quantitative comparison with experiments.

In order to better discern the mechanisms leading to the shear-induced diffusion, we calculated the power spectrum (PS) of the components of the trajectories for fixed  $\phi$  and  $Re$ , as can be seen respectively from Figs. 2 and 3. In Fig. 2(a), we present the PS of  $x(t)$  for four different values of  $Re$  and  $\phi=0.14$ . The insets represent three different trajectories for the same particle with the same initial condition for  $Re=0.01, 0.07$ , and  $0.08$ . For the lowest Reynolds number (solid line), the PS presents more pronounced peaks located at the excitation frequency and its harmonics. The trajectory in the inset (i) (solid line) corresponds to this spectrum and shows a very regular behavior. From the PS for the case of  $Re=0.04$  (dotted line) it follows that the dynamics in the  $x$  component keeps the main peak and harmonics at the same position than in the previous case, but small peaks start to appear between the harmonics. This is a consequence of the hydrodynamic interactions between the particles that give rise to new frequencies in the dynamics of the system. In the case  $Re=0.07$  (dashed line) there is a shift of the harmonics and the new frequencies are better defined. The corresponding trajectory (dashed line) is shown in the inset (ii). Finally, for  $Re=0.08$  (short-dashed line) the harmonics disappear and the energy is more homogeneously distributed for frequencies larger than the one imposed. The corresponding trajectory (dotted line), shown in the inset (iii), is irregular. In Fig. 2(b) we present the PS corresponding to the  $y$  movement of the particle for different  $Re$  at a fixed  $\phi$ . From this set of PS we can appreciate that both the  $x$  and  $y$  movements are coupled with the exciting frequency, as well as the fact that the harmonics have a small shift and the energy is distributed in more frequencies. The PS of  $x(t)$  and  $y(t)$  shown in Figs. 2(a) and 2(b) agree with theoretical results in two ways. First, they indicate a coupling between different modes, as in Eq. (37). Second, the power spectra reflect that hydrodynamic interactions become important only for Reynolds numbers larger than a certain value, as established by Eq. (41).

The theoretical results (35) and (39) indicate that the shear-induced effect is caused by hydrodynamic interactions and, although it is not explicitly shown, one then expects that the effect also depends on particle concentration. This was confirmed by performing another set of simulations keeping  $Re=0.08$  constant and varying  $\phi$  to analyze the influence of hydrodynamic interactions on the dynamics of the particles through the PS of  $x(t)$  and  $y(t)$ . The results are shown in Figs. 3(a) and 3(b), respectively. For the lower volume fraction  $\phi=0.00636$  (one particle) the PS for  $x(t)$ , Fig. 3(a), has only one peak at the exciting frequency. This result is expected from theory, Eq. (40), since for sufficiently small strains and frequencies the leading contribution corresponds to the first term on the right-hand side, which is proportional to the applied strain. For the  $y(t)$ , Fig. 3(b), the peak is shifted to the right from the exciting frequency, showing a weak coupling between the  $x$  and  $y$  motions. For  $\phi$

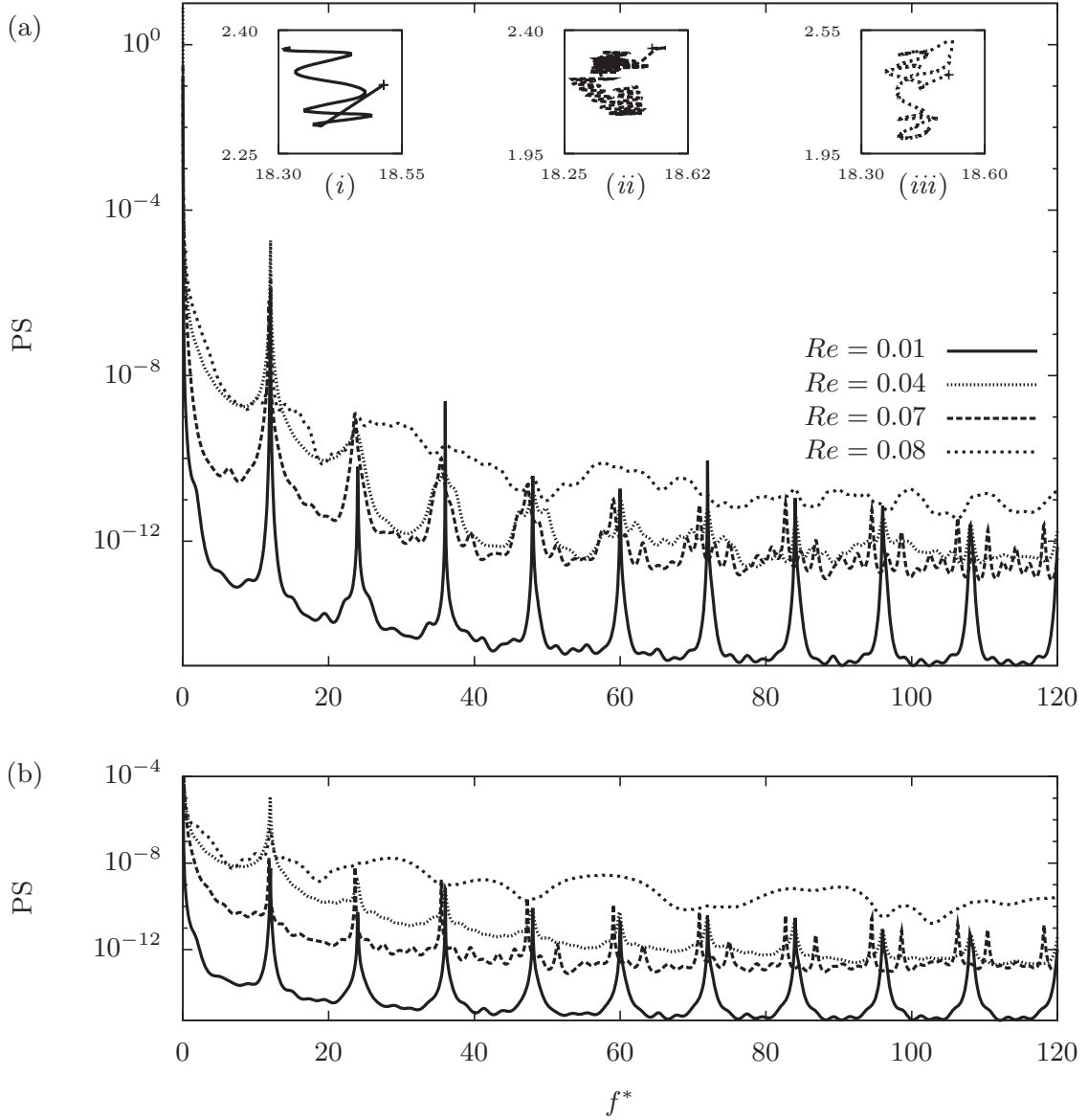


FIG. 2. Power spectrum for the same particle at different Reynolds numbers for (a) the  $x$  and (b) the  $y$  movement. The cross in the insets indicates the initial position of the particle, the same in the three cases. Notice that maximum displacement increases with increasing Reynolds number.

$=0.01270$  (two particles),  $x(t)$  presents harmonics which disappear at frequencies much larger than the exciting one whereas for  $y(t)$  the peak at the exciting frequency appears with an incipient presence of harmonics, implying that hydrodynamic interactions are weak. For  $\phi=0.02540$  (four particles) three harmonics can be identified for both  $x(t)$  and  $y(t)$ . For  $\phi=0.05090$  (eight particles) a larger number of harmonics can be identified in  $x(t)$  with about half of the energy in comparison with the exciting frequency. For the  $y(t)$ , the harmonics are clearly identified and have the same energy as the exciting frequency. New frequencies arise between the harmonics implying that hydrodynamic interactions introduce new modes in the dynamics of the particles. This result is expected from the evolution equation (40) which predicts that, for strains or particle concentrations larger than a certain critical value, new modes will appear in the behavior of  $\vec{R}(t)$  due to the contributions of the nonlinear

terms. Finally, for  $\phi=0.102$  (16 particles), the only peak for  $x(t)$  and  $y(t)$  is located at the exciting frequency and the energy is now homogeneously distributed in more frequencies. These results indicate that an increase in particle concentration enhances the effects of hydrodynamic interactions, which in turn are responsible for distributing the energy in a growing number of modes. They also reflect the fact that hydrodynamic interactions also introduce a dependence on volume fraction through the dependence on the volume fraction of the coefficients  $\tilde{\mu}_{xy}(\phi)$  and  $E(\phi)$ .

## V. CONCLUSIONS

In this paper, we have analyzed the shear-induced diffusion effect in suspensions under oscillatory shear by means of a thermokinetic theory based on the calculation of the

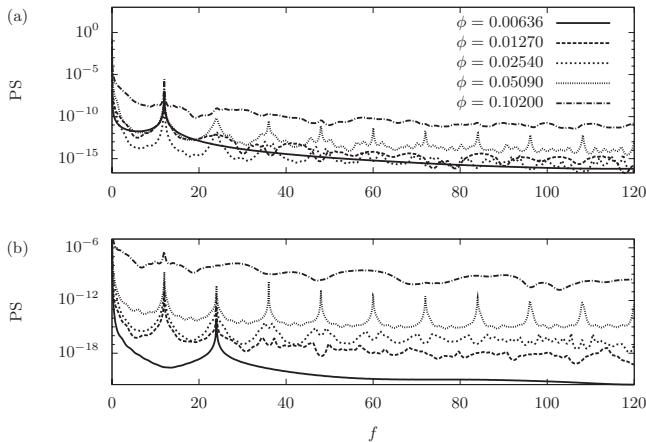


FIG. 3. Power spectrum for different values of  $\phi$  at  $Re=0.08$  for (a) the  $x$  and (b) the  $y$  movement of the trajectory of a particle.

entropy production at the mesoscopic level. We have found that an Onsager coupling between thermal and nonthermal effects containing hydrodynamic interactions is responsible for this effect.

By calculating the entropy production of the  $N$ -particle system in contact with a heat bath and identifying the corresponding forces and currents, we have derived a Fokker-Planck equation for the  $N$ -particle phase space distribution function having an effective diffusion coefficient in which the coupling between thermal and nonthermal effects breaks the validity of the fluctuation-dissipation theorem. After contracting the description over velocity space, assuming that the diffusion regime is well established and using an effective medium approximation, we derived a Smoluchowski equation for the single-particle distribution function containing an effective diffusion tensor incorporating the cross effects of the imposed flow and hydrodynamic interactions, Eq. (32). In the limit  $k_B T/m \rightarrow 0$ , this diffusion tensor yields the same scaling on particle diameter and applied strain as found in experiments and simulations,  $D \approx d^2 \tilde{\mu}_{xy}(\phi) [E(\phi) - 1] \gamma_0/6$ . Our analysis may also explain the influence thermal noise on this effect.

The lattice-Boltzmann simulations we performed were used to show in more detail the dependence of the shear-induced diffusion on the Reynolds number and the particle volume fraction. To this effect we have used the power spectrum of the components of particle trajectories. As expected from theory, we found a linear dependence of the diffusion coefficient  $D_{\text{eff}}$  as a function of the Reynolds number  $Re$ . When  $Re$  is increased for fixed  $\phi$  as well as  $\phi$  for fixed  $Re$ , we obtained that the power spectrum shows an increasing contribution of new modes, period doubling, and finally, for large  $Re$  and  $\phi$ , a loss of characteristic frequencies indicating a stochastic behavior induced by hydrodynamic interactions, in accordance with theoretical results expressed through the mean square displacement (39). It is important to emphasize that the 2D simulations performed clearly indicate that up to intermediate volume fractions the hydrodynamic interactions are responsible for the shear-induced diffusion effect, in agreement with the theoretical prediction. A more precise description could be carried out from 3D simulations in order to perform a quantitative comparison with experiments.

The expression for the shear-induced diffusion coefficient in Eq. (39) and the condition (41) show that the transition to irreversibility is due to hydrodynamic interactions and that it depends on the volume fraction, in accordance with experiments and theoretical simulations. Therefore, our study gives a theoretical explanation of the shear-induced effect and the transition to irreversibility based on the pertinent analysis of the entropy production at mesoscopic level, and therefore shows that the irreversibility inherent to the chaotic behavior of the macroscopic motions of the particles is perfectly compatible with the second law of thermodynamics.

#### ACKNOWLEDGMENTS

We acknowledge Professor D. J. Pine for interesting discussions on experiments, Dr. R. Rechtman for valuable commentaries on the numerical simulations, and Dr. G. Ruiz Chavarría for technical support. G.B.V. acknowledges financial support by DGAPA-UNAM and I.S.H. support by Grant No. DGAPA-IN102609.

- 
- [1] D. J. Pine, J. P. Gollub, J. F. Brady, and A. M. Leshansky, *Nature (London)* **438**, 997 (2005).
  - [2] G. Drazer, J. Koplik, B. Khusid, and A. Acrivos, *J. Fluid Mech.* **460**, 307 (2002).
  - [3] V. Breedveld, D. van den Ende, A. Tripathi, and A. Acrivos, *J. Fluid Mech.* **375**, 297 (1998).
  - [4] G. I. Taylor and J. Friedman, *Low Reynolds Number Flows*, National Committee on Fluid Mechanics Films (Encyclopedia Britannica Educational Corp., United States, 1996).
  - [5] A. Seriou and J. F. Brady, *J. Fluid Mech.* **506**, 285 (2004).
  - [6] G. Boffeta, M. Cencini, M. Falcioni, and A. Vulpiani, *Phys. Rep.* **356**, 367 (2002).
  - [7] I. Santamaría-Holek, D. Reguera, and J. M. Rubi, *Phys. Rev. E* **63**, 051106 (2001).
  - [8] I. Santamaría-Holek, J. M. Rubi, and A. Pérez-Madrid, *New J. Phys.* **7**, 35 (2005).
  - [9] D. Reguera, J. M. G. Vilar, and J. M. Rubi, *J. Phys. Chem. B* **109**, 21502 (2005).
  - [10] R. Zwanzig, *Adv. Chem. Phys.* **15**, 325 (1969).
  - [11] W. V. Saarloos and P. Mazur, *Physica A* **120**, 77 (1983); C. W. J. Beenakker, W. V. Saarloos and P. Mazur, *ibid.* **127**, 451 (1984).
  - [12] M. López de Haro and J. M. Rubi, *J. Chem. Phys.* **88**, 1248 (1987).
  - [13] L. Yeomans-Reyna, H. Acuña-Campa, and M. Medina-Noyola, *Phys. Rev. E* **62**, 3395 (2000).
  - [14] J. M. Rubi and P. Mazur, *Physica A* **250**, 253 (1998).
  - [15] G. Ryskin, *Phys. Rev. Lett.* **61**, 01442 (1988).
  - [16] R. Mauri and D. Leporini, *Europhys. Lett.* **76**, 1022 (2006).
  - [17] S. Sarman, D. J. Evans, and A. Baranyai, *Phys. Rev. A* **46**, 893 (2005).

- (1992).
- [18] Y. Drossinos and M. W. Reeks, *Phys. Rev. E* **71**, 031113 (2005).
- [19] G. Subramanian and J. F. Brady, *Physica A* **334**, 343 (2004).
- [20] A. V. Popov and R. Hernandez, *J. Chem. Phys.* **126**, 244506 (2007).
- [21] R. Rodríguez, E. Salinas-Rodríguez, and J. Dufty, *J. Stat. Phys.* **32**, 279 (1983).
- [22] J. V. Sengers and J. M. Ortiz de Zárate, *J. Non-Equil. Thermodyn.* **32**, 319329 (2007).
- [23] S. R. de Groot and P. Mazur, *Non-Equilibrium Thermodynamics* (Dover, New York, 1984).
- [24] J. W. Dufty and J. M. Rubi, *Phys. Rev. A* **36**, 222 (1987).
- [25] P. Mazur and D. Bedeaux, *Physica (Utrecht)* **76**, 235 (1974).
- [26] J. Happel and H. Brenner, *Low Reynolds Number Hydrodynamics* (Kluwer Academic, Dordrecht, 1991).
- [27] G. Bossis and J. F. Brady, *J. Chem. Phys.* **91**, 1866 (1989).
- [28] K. F. Freed and M. Muthukumar, *J. Chem. Phys.* **69**, 2657 (1978).
- [29] M. Mayorga, L. Romero-Salazar, and J. M. Rubi, *Physica A* **307**, 297 (2002).
- [30] T. L. Hill, *An Introduction to Statistical Thermodynamics* (Dover, New York, 1986).
- [31] Y. Qian, D. d'Humieres, and P. Lallemand, *Europhys. Lett.* **17**, 479 (1992).
- [32] P. L. Bhatnagar, E. P. Gross, and M. Krook, *Phys. Rev.* **94**, 511 (1954).
- [33] X. He and L. S. Luo, *Phys. Rev. E* **56**, 6811 (1997).
- [34] C. K. Aidun, Y. Lu, and E. J. Ding, *J. Fluid Mech.* **373**, 287 (1998).
- [35] A. J. C. Ladd, *J. Fluid Mech.* **271**, 285 (1994); **271**, 311 (1994).